Calculation of Raman intensities for the ringpuckering vibrations of trimethylene oxide and cyclobutane. The importance of electrical anharmonicity

David F. Bocian, G. Alan Schick, and Robert R. Birge

Citation: The Journal of Chemical Physics **74**, 3660 (1981); doi: 10.1063/1.441592
View online: http://dx.doi.org/10.1063/1.441592
View Table of Contents: http://scitation.aip.org/content/aip/journal/jcp/74/7?ver=pdfcov
Published by the AIP Publishing

Calculation of Raman intensities for the ring-puckering vibrations of trimethylene oxide and cyclobutane. The importance of electrical anharmonicity

David F. Bocian,[a] G. Alan Schick, and Robert R. Birge

Department of Chemistry, University of California, Riverside, California 92521
(Received 27 October 1980; accepted 18 December 1980)

Raman intensities are calculated for the ring-puckering vibration of trimethylene oxide (TMO) and cyclobutane using an anisotropic atom–point dipole interaction model to calculate the elements of the molecular polarizability tensor. Three different models for the ring-puckering motion are examined: (i) a model in which the methylene groups are held rigid to the molecular frame as the ring puckers, (ii) a dynamical model in which the methylene groups rock (TMO and cyclobutane) and wag (TMO) as the ring puckers, and (iii) a second rigid model in which all of the polarizability of the molecule is localized on the atoms of the ring skeleton. All three models for the ring-puckering motion predict unusually large second-order terms in the expansion of the polarizability tensor elements in the ring puckering coordinate $[|(\partial^2\alpha_{\mu\nu}/\partial Z^2)_0|>0]$. These terms result in intense $\Delta v=2$ overtone transitions. The calculated relative intensities of the members of the $\Delta v=2$ overtone progression are in good agreement with those observed for both molecules. The calculations also predict that for TMO the intensities of the $\Delta v=2$ overtones are comparable to the $\Delta v=1$ fundamentals. This result when evaluated in terms of the expected differences in the band shapes of the two types of transitions readily accounts for the predominance of the overtone transitions in the Raman spectrum of TMO.

I. INTRODUCTION

The low-frequency (<400 cm^{-1}) out-of-plane bending deformations of small ring molecules have been the subject of extensive investigation.[1–5] It has been found that the ring-puckering motion of four-membered rings, five-membered rings containing one double bond and six-membered rings containing two double bonds is generally large in amplitude and very anharmonic. Nonetheless, the motion is well described by a simple potential function of the form $V(Z)=aZ^4+bZ^2$, where Z is the ring-puckering coordinate.[2] The equilibrium conformation of the ring is planar if the constant $b>0$ or if $b<0$ and the ratio $|b|/a\ll 1$. The equilibrium conformation is puckered if $b<0$ and the ratio $|b|/a$ is not small.

Planar and nonplanar ring molecules with effective C_{2v} symmetry have a nonzero dipole moment derivative with respect to the ring-puckering coordinate $[(\partial\mu_i/\partial Z)_0\neq 0]$, so the vibration is infrared allowed (B_1 symmetry). The puckering motion is generally directed along the C axis of inertia and the gas-phase far-infrared spectrum of the molecule is characterized by a progression of sharp Q-branches due to $\Delta v=1$ transitions which occur from the ground state and from a number of thermally populated excited vibrational levels of the low-energy mode.[2] These ring-puckering transitions are also Raman allowed for molecules with effective C_{2v} symmetry $[(\partial\alpha_{\mu\nu}/\partial Z)_0\neq 0$, where $\alpha_{\mu\nu}$ is a component of the molecular polarizability tensor$]$, and it is expected that a progression of $\Delta v=1$ transitions could also be observed in the gas-phase Raman spectra of these molecules. Invariably, however, the $\Delta v=1$ transitions are absent in the Raman spectrum and only a progression of $\Delta v=2$ overtones (A_1 symmetry) is observed.[3]

One possible explanation for the absence of the $\Delta v=1$ transitions in the Raman spectrum is that these non-totally symmetric vibrations are expected to have weak Q-branches and broad band contours which could overlap and obscure any prominent features in the spectrum. In contrast, the totally symmetric $\Delta v=2$ overtones are expected to exhibit sharp well-defined Q-branches.[6,7] It has also been suggested, however, that the dominance of the $\Delta v=2$ transitions in the Raman spectrum is in large part due to unusually large second-order terms in the expansion of the polarizability tensor elements in the ring-puckering coordinate $[|(\partial^2\alpha_{\mu\nu}/\partial Z^2)_0|>|(\partial\alpha_{\mu\nu}/\partial Z)_0|]$.[3] These so-called "electrically anharmonic" terms could become large because of the large-amplitude of the ring-puckering motion and give rise to unusually intense $\Delta v=2$ overtones which could obscure the $\Delta v=1$ transitions. Thus far, polarizability expansions for the ring-puckering motion have not been calculated explicitly and the relative importance of the higher-order terms is not accurately known.

In this paper we report the calculation of the Raman intensities for the ring-puckering transitions of the four-membered rings trimethylene oxide (TMO) and cyclobutane. A series of $\Delta v=2$ ring-puckering transitions is observed in the gas-phase Raman spectrum of both molecules.[8–10] The $\Delta v=1$ ring-puckering transitions are forbidden in cyclobutane $[(\partial\alpha_{\mu\nu}/\partial Z)_0=0]$ which has effective D_{4h} symmetry but are allowed in the oxygen containing molecule which has effective C_{2v} symmetry. Thus, the relative intensities (neglecting differences in the band shapes) of the $\Delta v=1$ and $\Delta v=2$ transitions can be directly compared for TMO. The molecular polarizabilities for the two molecules are calculated using an anisotropic atom-point dipole interaction (AAPDI) model recently developed by Birge.[11] This model has been found to be much more effective than simple iso-

[a] Author to whom correspondence should be addressed.

 0021-9606/81/073660-08$01.00

tropic atom-point dipole models for calculating the average polarizability and polarizability anisotropy of small polyatomic molecules. We first review the salient features of the AAPDI model and discuss the general form of the polarizability expansions and the origin of the Raman intensities for the ring-puckering transitions. We then present the calculation of the Raman intensities for several different models of the ring-puckering motion. We find that the calculated intensities of the $\Delta v = 2$ overtones are in good agreement with those observed for both molecules. We also find that the intensities of the $\Delta v = 2$ transitions in TMO are comparable to those of the $\Delta v = 1$ transitions.

II. THEORETICAL SECTION

A. Anisotropic atom point dipole interaction model

A discussion of the AAPDI model used to calculate the molecular polarizability tensor as a function of geometry may be found in Ref. 11. The AAPDI model is based on the point dipole interaction model developed by Silberstein,[12] and the more recent formalistic and parametric modifications introduced by Applequist, Carl, and Fung[13] which permit the calculation of polarizability tensors of polyatomic molecules. The procedures and parametrization developed by Applequist and co-workers yield a model capable of predicting average molecular polarizabilities with errors comparable to experiment (approximately 3%).[13] The use of isotropic atom polarizabilities within these procedures, however, leads to significant errors in the calculated molecular polarizability components and anisotropies.

Although the isotropic atom procedures are relatively successful at calculating the mean polarizability derivatives as a function of nuclear displacement, they are less successful at calculating the corresponding anisotropies.[14] Because the latter functions are of critical importance to the accurate calculation of electrical anharmonicity (see below), we have adopted the AAPDI procedures developed by Birge.[11] We now briefly review the principal procedures and assumptions that are inherent in the AAPDI model, concentrating on those aspects of the model which are of primary importance to the objective at hand, namely, the accurate prediction of the components of the molecular polarizability tensor.

The AAPDI model differs from the isotropic atom procedures of Applequist and co-workers in only one important respect. Instead of calculating the molecular polarizability tensor as a point dipole interaction involving isotropic atoms, the AAPDI model calculates an atomic polarizability tensor for each atom based on its molecular environment prior to performing a point-dipole interaction analysis.

The environmental anisotropy is introduced by means of a symmetric second-rank tensor

$$\Gamma^{A}_{\mu\nu} = \sum_{B\,(\neq A)}^{N} [\bar{\alpha}_B (g_{AB})^{\kappa} (\mu\nu / r^2_{AB})] , \tag{1}$$

where the sum extends over all N atoms in the molecule not including atom A, $\Gamma^{A}_{\mu\nu}$ is the (μ, ν)th component of the Cartesian tensor for atom A, $\bar{\alpha}_B$ is the average polarizability of atom B, g_{AB} is the electronic repulsion integral associated with atoms A and B, κ is the repulsion exponent (see below), μ and ν (on the right-hand side) are the Cartesian components of the vector connecting atoms A and B, and r_{AB} is the internuclear separation.

We approximate the electronic repulsion integral associated with atoms A and B using the Ohno formula[15]

$$g_{AB} = 14.397 / \{[2(14.397)/(g_{AA} + g_{BB})]^2 + r^2_{AB}\}^{1/2} , \tag{2}$$

where g_{AA} and g_{BB} are one-center repulsion integrals appropriate for the valence states of atoms A and B, respectively. It should be noted that the accuracy of the calculated molecular polarizability anisotropies is not very sensitive to the accuracy of the electron repulsion integral.[11]

Normalization of the Γ tensor yields the "normalized atomic anisotropy tensor"

$$G^{A}_{\mu\nu} = \eta^{A} \Gamma^{A}_{\mu\nu} , \tag{3}$$

where

$$\eta^{A} = 3/(\Gamma^{A}_{xx} + \Gamma^{A}_{yy} + \Gamma^{A}_{zz}) . \tag{4}$$

The G tensor is normalized such that the average diagonal element is equal to unity (TrG = 3). The diagonal elements of the valence state polarizability tensor for atom A are given by

$$\alpha^{A}_{\mu\mu} = \bar{\alpha}_A [1 + \xi_A (1 - G^{A}_{\mu\mu})] \tag{5}$$

and the off-diagonal elements are given by

$$\alpha^{A}_{\mu\nu} = -\bar{\alpha}_A \xi_A G^{A}_{\mu\nu} \quad (\mu \neq \nu) , \tag{6}$$

where ξ_A is a dimensionless atomic anisotropy constant which is appropriate for a given atom in a particular molecular environment.

Equations (1)–(6) specify the procedures for calculating the atomic polarizability tensor in a molecular environment. One of the most important features of this formalism is that all of the calculated atomic and molecular (observable) properties are invariant to coordinate transformations. In other words, the calculated principal components of the atomic and molecular polarizabilities are invariant to the chosen orientation of the molecule used in the calculation (the unit vectors which define the principal axes of the polarizability are, of course, determined by the orientation of the molecule in space).

The atomic anisotropy constant ξ_A and the repulsion exponent κ are treated as adjustable parameters which are optimized to produce the best fit to experimental molecular polarizability anisotropies. A discussion of the optimization procedures may be found in Ref. 11. The parameters used for the present calculations are

$$\bar{\alpha}^0_H = 0.135 \text{ Å}^3, \quad \xi_H = 0.430, \quad g_{HH} = 12.848 \text{ eV},$$
$$\bar{\alpha}^0_C = 0.878 \text{ Å}^3, \quad \xi_C = 0.347, \quad g_{CC} = 10.333 \text{ eV},$$
$$\bar{\alpha}^0_O = 0.465 \text{ Å}^3, \quad \xi_O = 0.184, \quad g_{OO} = 13.907 \text{ eV}$$
$$\kappa = 2.8 \qquad \text{(from Table I of Ref. 11)},$$

where the $\bar{\alpha}^0_A$ are the average atomic polarizabilities

for *isotropic* atoms. These average polarizabilities must be reoptimized for each molecular geometry (see below).

The calculation of the molecular polarizability tensor as a function of the atomic polarizability tensors defined using Eqs. (5) and (6) proceeds by evaluating the following matrix for a molecule containing N atoms:

$$\mathbf{A}=\begin{bmatrix} \boldsymbol{\alpha}_1^{-1} & \mathbf{T}_{12}\cdots\mathbf{T}_{1N} \\ \mathbf{T}_{21} & \boldsymbol{\alpha}_2^{-1}\cdots\mathbf{T}_{2N} \\ \vdots & \\ \mathbf{T}_{N1} & \mathbf{T}_{N2}\cdots\boldsymbol{\alpha}_N^{-1} \end{bmatrix} \tag{7}$$

where $\boldsymbol{\alpha}_A^{-1}$ is the inverse of the polarizability tensor of atom A, and $\mathbf{T}_{AB}$ is the dipole field tensor

$$\mathbf{T}_{AB}=(r_{AB}^{-3})\,\mathbf{I}-3(r_{AB}^{-5})\begin{bmatrix} x^2 & xy & xz \\ yx & y^2 & yz \\ zx & zy & z^2 \end{bmatrix} . \tag{8}$$

The **A** matrix is then inverted to produce the relay tensor matrix **B**,

$$\mathbf{B}=\mathbf{A}^{-1}=\begin{bmatrix} \mathbf{B}_{11} & \mathbf{B}_{12}\cdots\mathbf{B}_{1N} \\ \mathbf{B}_{21} & \mathbf{B}_{22}\cdots\mathbf{B}_{2N} \\ \vdots & \\ \mathbf{B}_{N1} & \mathbf{B}_{N2}\cdots\mathbf{B}_{NN} \end{bmatrix} \tag{9}$$

which is a partitioned matrix with 3×3 elements $\mathbf{B}_{AB}$. The molecular polarizability tensor is the sum of these 3×3 elements:

$$\boldsymbol{\alpha}_{\mathrm{mol}}=\sum_{A=1}^{N}\sum_{B=1}^{N}\mathbf{B}_{AB} . \tag{10}$$

Diagonalization of α_{mol} yields eigenvalues which are the principal components of the polarizability $\alpha'_{\mathrm{mol}}(=\alpha_1,\alpha_2,\alpha_3)$ and the unit eigenvectors which define the directions of the principal components with respect to the Cartesian coordinates of the molecule.

Unfortunately, the average atomic polarizabilities ($\bar{\alpha}_A^0$) listed by Applequist *et al.* are generally not optimal for use in Eqs. (1)–(6). The mean atomic polarizabilities required for the AAPDI model are invariably larger than those which were determined by Applequist and co-workers to be optimal for the isotropic model. Accordingly, it is necessary to reoptimize the average atomic polarizabilities $\bar{\alpha}_A$.

The most straightforward approach to reoptimization of the average atomic polarizabilities is to iteratively adjust the $\bar{\alpha}_A$ values to generate identical mean molecular polarizabilities as calculated by the isotropic model. Although these iterative procedures (which must be carried out for each molecular geometry separately) require additional computer time, they have the significant advantage of introducing atomic anisotropy without diminishing the accuracy of the calculated mean molecular polarizabilities obtained using the optimized isotropic model of Ref. 13. Details of the procedures used to iteratively adjust the average atom polarizabilities are given in Ref. 11. It is sufficient to note for the purposes of the present discussion that the AAPDI model predicts components of the molecular polarizability tensor with an average error of ~7%. This error is comparable to experimental uncertainty.

A potential source of confusion is associated with the iterative procedures discussed above. It should be emphasized that the $\bar{\alpha}_A^0$ parameters represent the average atomic polarizabilities that are appropriate for isotropic atom calculations. The mean molecular polarizability of the molecule is calculated by assuming isotropic atoms ($\xi_A=0$ and $\alpha_{xx}^A=\alpha_{yy}^A=\alpha_{zz}^A=\bar{\alpha}_A^0$). The iterative procedures subsequently adjust the mean molecular polarizability to match the isotropic calculation by using $\bar{\alpha}_A^0$ as an initial guess. The algorithms for carrying out this process are fairly complex and are fully described in Ref. 11. The reason the iterative procedures must be carried out for each molecular geometry is because the components of the anisotropy tensor [Eq. (1)] are dependent on the conformation.

One inherent limitation in the AAPDI model is the assumption that the total molecular polarizability can be described as the interaction of point dipoles. It would certainly be preferable to calculate polarizabilities by accounting for the distribution of electron density which occurs in the molecular system. This approach has been demonstrated by other investigators to significantly improve the theoretical prediction of molecular polarizability tensors.[16,17] However, the computational complexity of these procedures precludes their application to molecules of the size investigated here. The improper treatment of the hydrogen atoms may represent the most severe constraint on the applicability of our localized point dipole procedures because the electron density of hydrogen will be significantly shifted from the nuclear center. We will discuss this limitation in more detail in Sec. III C where we calculate the Raman intensities for the ring-puckering vibrations of TMO and cyclobutane using a model which neglects the contributions of the hydrogen atoms to the molecular polarizability expansion. A comparison of these calculations with those which explicitly include the hydrogen atoms clearly shows that the principal observations of this study are not an artifact of a localized point dipole model.

B. Origin of the Raman intensity

The intensity of a Stokes Raman transition is given by the following expression[18]:

$$I_{v'',v'}=N(\bar{\nu}_0-\bar{\nu})^4\frac{e^{-h\bar{\nu}c/kT}}{Q}\left(\frac{45\bar{\alpha}_{v'',v'}^2+7\gamma_{v'',v'}^2}{45}\right) , \tag{11}$$

where v'' and v' are the initial and final vibrational states, N is a constant, $\bar{\nu}_0$ and $\bar{\nu}$ are the frequencies of the incident radiation and the vibrational mode, Q is the partition function, and $\bar{\alpha}$ and γ^2 are the invariants of the molecular polarizability tensor, defined by

$$\bar{\alpha}=\tfrac{1}{3}(\alpha_{xx}+\alpha_{yy}+\alpha_{zz}) , \tag{12}$$

$$\gamma^2=\tfrac{1}{2}[(\alpha_{xx}-\alpha_{yy})^2+(\alpha_{yy}-\alpha_{zz})^2+(\alpha_{zz}-\alpha_{xx})^2+6(\alpha_{xy}^2+\alpha_{yz}^2+\alpha_{zx}^2)] . \tag{13}$$

The standard expansion[6] of the elements of the polarizability tensor in a Taylor series in the vibrational coordinate Z results in the following expression for any element $\alpha_{\mu\nu}(\mu\nu = x, y, z)$:

$$\alpha_{\mu\nu} = \alpha^0_{\mu\nu} + (\partial\alpha_{\mu\nu}/\partial Z)_0 Z + \tfrac{1}{2}(\partial^2\alpha_{\mu\nu}/\partial Z^2)_0 Z^2 + \cdots . \quad (14)$$

The corresponding matrix elements for the transition $v' - v''$ are

$$[\alpha_{\mu\nu}]_{v''v'} = \left(\frac{\partial\alpha_{\mu\nu}}{\partial Z}\right)_0 \langle v''|Z|v'\rangle + \frac{1}{2}\left(\frac{\partial^2\alpha_{\mu\nu}}{\partial Z^2}\right)_0 \langle v''|Z^2|v'\rangle + \cdots . \quad (15)$$

Normally, the first term in Eq. (15) is much larger than any of the higher-order terms when the transition is first-order allowed.[18] The result is the appearance of $\Delta v = 1$ transitions in the Raman spectrum. When the vibrational motion is anharmonic, overtone transitions can also obtain intensity from the first term in Eq. (15). Note, however, that overtone transitions can arise from this term only when the fundamental transition is allowed $[(\partial\alpha_{\mu\nu}/\partial Z)_0 \neq 0]$. The contribution of mechanical anharmonicity is generally the major source of intensity for overtone transitions.[6,18]

Overtone transitions can also obtain intensity from the second- and higher-order terms in Eq. (15). These terms can give rise to overtones even when the fundamental is not allowed. The evidence that second-order terms are substantial for the ring-puckering motion in molecules with C_{2v} or higher effective symmetry is the observation of $\Delta v = 2$ overtones itself. This is apparent from the symmetry of the eigenfunctions of the quartic–quadratic potential function which describes the ring-puckering motion.[19,20] These eigenfunctions are either symmetric or antisymmetric with respect to inversion through the plane of the ring. Accordingly, the first term in Eq. (15) can only contribute to transitions for which v'' and v' are of opposite parity $(\Delta v = 1, 3, 5\ldots)$. Similarly, the second-order term can only contribute to transitions for which v'' and v' are of the same parity $(\Delta v = 2, 4, 6, \ldots)$. The observation of $\Delta v = 2$ overtones for the ring-puckering motion of molecules with C_{2v} or higher effective symmetry must then reflect the occurrence of substantial second-order terms.

III. CALCULATION OF THE POLARIZABILITY EXPANSIONS AND RAMAN INTENSITIES FOR THE RING-PUCKERING TRANSITIONS OF TMO AND CYCLOBUTANE

The expansions of the elements of the polarizability tensor in terms of the ring-puckering coordinate were obtained by calculating the polarizability (see Sec. IIA) for conformations of the ring ranging from $Z = 0$ (planar) to $Z = 0.15$ Å in steps of 0.01 Å and then fitting the calculated values of the $\alpha_{\mu\nu}$ to power series using a nonlinear least squares procedure. The atomic Cartesian coordinates used in the polarizability calculations were obtained from the geometrical parameters of the molecule in the various conformations. The reference coordinate system in which the atomic displacements for the ring-puckering motion were evaluated is the principal axis system of the planar ring. The z axis for both cyclobutane and TMO is defined as being coincident with the out-of-plane axis of inertia. The choice of the x and y axes for cyclobutane is completely arbitrary because of symmetry, but for convenience these axes were defined as being coincident with the ring diagonals. The x and y axes for TMO were chosen such that the x axis is coincident with the inertial axis which lies along the oxygen–β-carbon diagonal of the planar ring.

Several different models for the form of the ring-puckering motion were investigated. These are described in detail below. The same geometry was assumed in all of the models for the hypothetical planar form of the ring, which is the initial conformation used to determine the expansions of the $\alpha_{\mu\nu}$. The geometry of the hypothetical planar form of TMO was that predicted from the microwave data.[21] The planar form of cyclobutane was assumed to have the same bond lengths and HCH bond angles as those given in Ref. 22 for the puckered equilibrium conformation. Expansions of the $\alpha_{\mu\nu}$ for the puckering motion were also calculated starting with other geometries for the hypothetical planar ring for both molecules. These geometries had bond lengths and HCH and HCO (TMO only) bond angles which differed by several hundredths of an Å or several degrees, respectively, from those given in Refs. 21 and 22. These different geometries did not result in significant differences in the polarizability expansions.

The Raman intensities for the ring-puckering transitions were determined using the calculated expansions of the $\alpha_{\mu\nu}$ and Eqs. (11)–(13). The vibrational transition moments were evaluated for the various eigenfunctions of the appropriate quartic–quadratic oscillator which were obtained by diagonalizing the Hamiltonian $\mathcal{H} = (P_Z^2/2\mu) + aZ^4 + bZ^2$ in a 40×40 harmonic oscillator basis set. The values of μ, a and b were obtained for cyclobutane and TMO from Refs. 9 and 23, respectively.

As was previously noted, the Raman intensities of TMO and cyclobutane were calculated for several different models of the ring-puckering motion. The first model is one in which the methylene groups remain rigid as the ring bends, with the two hydrogen atoms remaining equidistant from the plane defined by the CCC (or CCO) bonds. The second model is dynamical in nature and allows the hydrogen atoms to rock (TMO and cyclobutane) and wag (TMO) as the ring puckers. The bond lengths and HCH bond angles are held fixed at their equilibrium values in both of these models. The final model is also one in which the bond lengths remain fixed as the ring bends. In this model, however, all of the polarizability of the molecule is assumed to be localized on the atoms of the ring skeleton. Schematic diagrams of the atomic motions associated with each of these models are depicted in Fig. 1. We now discuss each of the models.

A. Rigid methylene group model

A model in which the methylene groups are held rigid to the molecular frame as the ring bends is the simplest

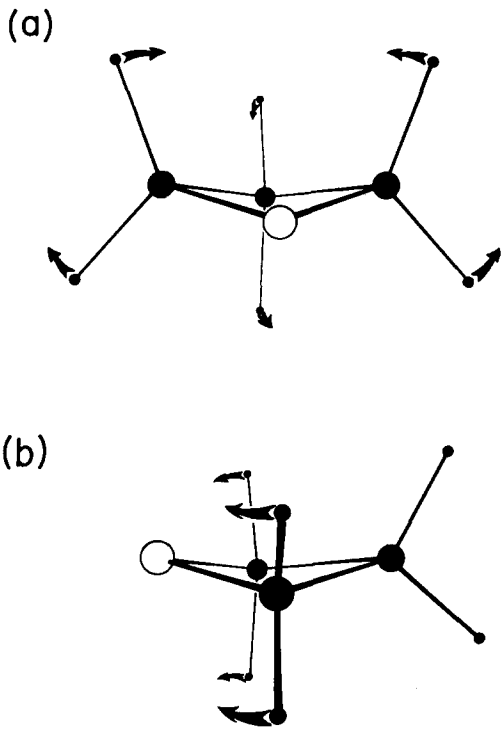

FIG. 1. Schematic representation of the (a) rocking and (b) wagging motions of the hydrogen atoms of TMO. The ring is shown in a puckered conformation where $Z = 0.10$ Å. Rocking is defined as the motion of both hydrogen atoms on a carbon atom C_i perpendicular to the plane defined by the atoms CC_iO or CC_iC in the same direction as the motion of atom C_i (the rocking motion for cyclobutane is defined in a similar fashion). Wagging is defined as the motion of both hydrogen atoms on an α-carbon atom parallel to the plane defined by the atoms CC_iO and toward the oxygen atom.

model for the ring-puckering motion. This model results in the following polarizability expansions for TMO:

$$\begin{aligned}
\alpha_{xx} &= 7.48 - 0.220Z^2 - 11.9Z^4 + \cdots , \\
\alpha_{yy} &= 6.97 + 8.64Z^2 - 105Z^4 + \cdots , \\
\alpha_{zz} &= 5.44 + 25.8Z^2 - 9.16Z^4 + \cdots , \\
\alpha_{zx} &= 7.35Z - 15.5Z^3 + \cdots ,
\end{aligned} \tag{16}$$

and cyclobutane:

$$\begin{aligned}
\alpha_{xx} = \alpha_{yy} &= 7.73 + 6.50Z^2 + 42.0Z^4 + \cdots , \\
\alpha_{zz} &= 5.88 + 19.1Z^2 + 45.0Z^4 + \cdots ,
\end{aligned} \tag{17}$$

where the units of $\alpha_{\mu\nu}$ and Z are Å^3 and Å, respectively, and the numerical coefficients have units which maintain consistency between the left and right-hand sides of the equations. Higher-order terms occur in the expansions for both molecules, but these are negligible compared to those listed above. All of the off-diagonal terms for cyclobutane and the terms α_{xy} and α_{yz} for TMO are zero by symmetry. The occurrence of a nonzero α_{zx} term for TMO (rather than α_{yz}) reflects the (arbitrary) location of the oxygen and β-carbon atoms in the xz plane.

The relative Raman intensities calculated for the ring-puckering transitions of TMO and cyclobutane using Eqs. (16) and (17) are listed in Tables I and II, respectively,

TABLE I. Calculated and observed Raman intensities for the ring-puckering transitions of TMO.

Transition	Frequency (cm^{-1})[a]	Relative intensity Calculated[b]	Relative intensity Observed[a]
		$\Delta v = 2$	
0–2	143.2	0.81	0.81
1–3	194.3	(1.0)	(1.0)
2–4	222.7	0.93	0.83
3–5	247.5	0.74	0.63
4–6	267.7	0.53	0.45
5–7	286.1	0.34	0.30
6–8	302.1	0.21	0.17
7–9	317.0	0.11	0.12
		$\Delta v = 1$	
0–1	53.4	22	···
1–2	89.9	19	···
2–3	104.7	16	···
3–4	118.1	11	···
4–5	128.8	6.9	···
5–6	138.9	4.1	···
6–7	147.1	2.2	···
7–8	155.0	1.1	···

[a]The frequencies and observed intensities of the $\Delta v = 2$ transitions were taken from Ref. 10(a). The intensities were estimated from the peak heights in Fig. 1 of this reference. The frequencies of the $\Delta v = 1$ transitions were taken from the far-infrared data reported in Ref. 23.
[b]Calculated using the rigid methylene group model.

along with the observed intensities. The calculated relative intensities of the members of the $\Delta v = 2$ progression for both molecules are in good agreement with those observed. The calculated intensities of the $\Delta v = 1$ transitions of TMO are 10–20 times greater than those

TABLE II. Calculated and observed Raman intensities for the ring-puckering transitions of cyclobutane.

Transition	Frequency (cm^{-1})[a]	Relative intensity Calculated[b]	Relative intensity Observed[a]
0–2[c], 1–3[c]	199.4	0.50, 0.50 (1.0)	(1.0)
2–4	159.3	0.28	0.32
3–5[c], 5–7[c]	177.1	0.33, 0.18 0.51	0.74
4–6	119.2	0.16	0.26
6–8[d]	174.5[d]	0.038	···
7–9[d]	204.5[d]	0.033	···

[a]The frequencies and observed intensities were taken from Ref. 9. The intensities were estimated from the peak heights in Fig. 1 of this reference. This method of determining the intensities may result in substantial errors for the overlapping bands.
[b]Calculated using the rigid methylene group model.
[c]These transitions are effectively degenerate because of the high barrier to planarity in cyclobutane.
[d]These transitions are not observed and the reported frequencies are calculated values.

of the $\Delta v = 2$ overtones. The single order of magnitude difference in the intensities of the fundamental and first overtone ring-puckering transitions of TMO is significantly less than that which occurs for small amplitude vibrations.[6] The strength of the overtone progression reflects the large second-order terms in Eq. (16), particularly the α_{zz} term which is several times larger than the first-order term for α_{zx}.

It is useful to compare the relative intensities of the $\Delta v = 1$ and $\Delta v = 2$ Raman transitions calculated using Eq. (16) to the relative intensities of these same transitions in the infrared. The $\Delta v = 2$ overtones are not observed in the far-infrared spectrum of TMO,[23] but their intensity can be approximated using a simple bond-dipole model. The expansions for the dipole moment can be determined in a manner identical to that used for the polarizabilities. Calculation of the infrared intensities using the expression given in Ref. 24 predicts that the $\Delta v = 1$ ring-puckering transitions are 100–200 times more intense than the $\Delta v = 2$ overtones. Thus, the $\Delta v = 2$ Raman overtone transitions are an order of magnitude more intense than the corresponding transitions in the infrared.

B. Dynamic methylene group models

It has been shown both experimentally[25–27] and theoretically[22,28–30] that the hydrogen atoms on opposing methylene groups in cyclobutane are rocked 3–6° toward each other (in the same direction as the ring is bent) in the puckered equilibrium form of the ring. This rocking motion allows the hydrogen atoms to attain a more staggered configuration (Fig. 1). It is not known whether the methylene groups of TMO also rock toward each other as the ring is bent away from the planar conformation. The barrier to planarity in TMO is very small (~15 cm^{-1})[23] compared to that of cyclobutane (~518 cm^{-1}),[8,9] and in the ground vibrational state the energy of the molecule exceeds the barrier height. Thus, the ring can be regarded as having an essentially planar equilibrium conformation in which no rocking is expected to occur. This does not, however, preclude the existence of a dynamical rocking motion of the methylene groups as the ring undergoes large amplitude inversion through the planar form.

Polarizability expansions and Raman intensities were calculated for the ring-puckering motion of both cyclobutane and TMO for a model in which the methylene groups rock linearly ($\propto aZ$) as the ring bends (nonlinear rocking[28] results in polarizability expansions which are negligibly different). The value of a was chosen to give 4° of rocking at $Z = 0.10$ Å, which is the amount of rocking predicted by theoretical calculations.[22] This value of Z corresponds to a dihedral angle of approximately 20°. It was found for both molecules that the inclusion of methylene rocking did not significantly affect the relative intensities of the members of the $\Delta v = 2$ overtone progression. The absolute intensities of these transitions were, however, greater than those of the rigid model.

The addition of the rocking motion to the ring pucker of TMO results in a significantly greater increase in the magnitude of the second-order diagonal components of the polarizability expansion than in the first-order off-diagonal α_{zx} element. The polarizability expansions calculated for TMO for this model are as follows:

$$\begin{aligned}
\alpha_{xx} &= 7.48 - 13.2Z^2 + 99.1Z^4 + \cdots , \\
\alpha_{yy} &= 6.97 + 6.81Z^2 + 163Z^4 + \cdots , \\
\alpha_{zz} &= 5.44 + 42.8Z^2 - 189Z^4 + \cdots , \\
\alpha_{zx} &= 8.36Z - 55.0Z^3 + \cdots .
\end{aligned} \tag{18}$$

The Raman intensities calculated with the expansions of Eq. (18) are compared with those of the rigid methylene group model in Table III. It can be seen that the inclusion of the rocking motion results in a substantial increase in the intensities of the $\Delta v = 2$ overtones relative to the $\Delta v = 1$ transitions. Here the overtones are only 5–10 times less intense than the fundamentals compared to the factor of 10–20 calculated for the rigid methylene group model.

TABLE III. Comparison of the calculated Raman intensities for the $\Delta v = 1$ and $\Delta v = 2$ ring-puckering transitions of TMO.

	Rigid model		Rocking model		Skeletal model	
v''	$\Delta v = 1$	$\Delta v = 2$	$\Delta v = 1$	$\Delta v = 2$	$\Delta v = 1$	$\Delta v = 2$
0	22	0.81	11	0.85	0.17	0.79
1	19	(1.0)	9.7	(1.0)	0.28	(1.0)
2	16	0.93	7.6	0.94	0.29	0.95
3	11	0.74	5.2	0.74	0.27	0.77
4	6.9	0.53	3.2	0.51	0.20	0.56
5	4.1	0.34	1.8	0.33	0.15	0.36
6	2.2	0.21	0.97	0.20	0.095	0.23
7	1.1	0.11	0.48	0.11	0.059	0.14

The final dynamical model for which Raman intensities were calculated is one in which the hydrogen atoms on the α-carbons of TMO wag toward the oxygen atom as the ring puckers. This type of motion has been suggested to occur in TMO on the basis of microwave spectroscopic data.[18] However, the uncertainties in these data preclude any definitive determination of the existence of such a motion. The model which we used for the wagging motion has a functional form which is symmetric about $Z = 0$ ($\propto aZ^2$), with a value of a chosen to give 5° of wagging[18] at $Z = 0.10$ Å. The Raman intensities calculated for this model were found to be nearly identical to those of the rocking model, although the exact values of the various coefficients of the polarizability expansions are quite different. These results suggest that both rocking and wagging motions can increase the intensities of the $\Delta v = 2$ overtones relative to the $\Delta v = 1$ transitions.

C. Skeletal model

As previously noted in Sec. II A, there is reason to believe that the AAPDI model may be incapable of accurately calculating the contributions to the polarizability expansion components associated with hydrogen motions. The AAPDI model may overestimate the contribution of these atoms to the expansion because it localizes the electron of the hydrogen atom at the position of

the atomic nucleus rather than between the hydrogen atom and the carbon to which it is bonded. The large amplitude puckering of the ring may then result in an exaggerated calculated motion of the electron density associated with the hydrogen atoms which could result in an anomalously large contribution to the polarizability expansion coefficients. In order to evaluate the importance of the motion of the hydrogen atoms to the polarizability expansions, we have carried out calculations in which these atoms are neglected. The skeletal model, therefore, calculates the polarizability expansions solely as a function of the motions of the carbon and oxygen (TMO) atoms. No other changes in the atomic parameterizations defined in Sec. II A are made.

The relative Raman intensities calculated for the members of the $\Delta v = 2$ progression of both TMO and cyclobutane using the skeletal model are similar to those calculated using the models which included the hydrogen atoms. However, the neglect of the hydrogen atoms in TMO results in extremely large differences between the first and second-order terms in the polarizability expansions, with $|(\partial^2 \alpha_{\mu\nu}/\partial Z^2)_0| \gg |(\partial \alpha_{\mu\nu}/\partial Z)_0|$. The polarizability expansions calculated for TMO using this model are as follows:

$$\begin{aligned} \alpha_{xx} &= 4.13 + 0.360Z^2 - 3.90Z^4 + \cdots , \\ \alpha_{yy} &= 3.91 - 0.730Z^2 + 0.500Z^4 + \cdots , \\ \alpha_{zz} &= 2.67 + 3.97Z^2 + 2.70Z^4 + \cdots , \\ \alpha_{zx} &= -0.050Z - 2.13Z^3 + \cdots . \end{aligned} \tag{19}$$

The Raman intensities calculated with these expansions are compared in Table III to those calculated with the other two models. The large differences in the first and second-order terms obtained with this model result in the $\Delta v = 2$ transitions which are 3–5 times *more intense* than the $\Delta v = 1$ transitions.

Since the AAPDI model may overestimate the contribution of the hydrogen atoms to the polarizability expansions, it is comforting to note that the neglect of these atoms results in an increase in the intensity of the already strong $\Delta v = 2$ overtones relative to the $\Delta v = 1$ transitions. This result suggests that the calculations which include the hydrogen atoms represent a lower limit for the calculated relative intensity of the $\Delta v = 2$ overtone and fundamental transitions. We therefore believe that the basic conclusions of this investigation are not founded on a mathematical artifact inherent in the AAPDI model, but on a real effect that is correctly predicted by the model.

IV. SUMMARY AND CONCLUSIONS

The polarizability expansions calculated for the ring-puckering motions of TMO and cyclobutane using any of the models discussed above result in calculated relative intensities for the $\Delta v = 2$ overtones in good agreement with those observed. This result is not altogether surprising since the intensity of these transitions depends only on the diagonal elements of the polarizability tensor which are dominated by the second-order term in the expansions. It does, however, further confirm the origin of these transitions.

The different models for the puckering motion in TMO all clearly indicate that the Raman overtones are extraordinarily intense and much more intense than their counterparts in the infrared. None of the models predict that the $\Delta v = 2$ overtones completely dominate the Raman spectrum, although the skeletal model does predict that these transitions are more intense than the $\Delta v = 1$ fundamentals. The skeletal model in all probability overestimates the intensity of the overtone transitions while the two models which include the hydrogen atoms underestimate their intensity. When all of the models are considered together, it appears that a reasonable estimate would be that the $\Delta v = 1$ and $\Delta v = 2$ transitions are comparable in intensity. This estimate when taken together with the expected differences in the band shapes for the two types of transitions readily accounts for the predominance of the overtone transitions in the Raman spectrum of TMO.

ACKNOWLEDGMENTS

This work was supported by the Donors of the Petroleum Research Fund (D. F. B.), administered by the American Chemical Society, Research Corporation (D. F. B.), the National Institutes of Health (R. R. B.), and the National Science Foundation (R. R. B.).

[1]Comprehensive reviews of gas-phase far-infrared and Raman studies of the puckering motion of small ring molecules can be found in Refs. 2 and 3, respectively.
[2]C. S. Blackwell and R. C. Lord, in *Vibrational Spectra and Structure*, edited by J. R. Durig (Dekker, New York, 1972), Vol. 1, pp. 1–24.
[3]C. J. Wurrey, J. R. Durig, and L. A. Carreira, in *Vibrational Spectra and Structure*, edited by J. R. Durig (Elsevier, New York, 1976), Vol. 5, pp. 121–277.
[4]J. Laane and R. C. Lord, J. Mol. Spectrosc. 39, 340 (1971).
[5]T. C. Rounds and R. C. Lord, J. Chem. Phys. 58, 4354 (1973).
[6]G. Herzberg, *Molecular Spectra and Structure* (Van Nostrand–Reinhold, New York, 1945), Vol. II.
[7]S. Brodersen, in *Raman Spectroscopy of Liquids and Gases*, edited by A. Weber (Springer–Verlag, Berlin, 1979), pp. 7–69.
[8]J. M. R. Stone and I. M. Mills, Mol. Phys. 18, 631 (1970).
[9]F. A. Miller and R. J. Capwell, Spectrochim. Acta 27A, 947 (1971).
[10](a) W. Kiefer, H. J. Bernstein, M. Danyluk, and H. Wiser, Chem. Phys. Lett. 12, 605 (1972); (b) J. Mol. Spectrosc. 43, 393 (1972).
[11]R. R. Birge, J. Chem. Phys. 72, 5312 (1980).
[12]L. Silberstein, Philos. Mag. 33, 92, 215, 521 (1917).
[13]J. Applequist, J. R. Carl, and K-K. Fung, J. Am. Chem. Soc. 94, 2952 (1972).
[14]J. Applequist, Accts. Chem. Res. 10, 79 (1977).
[15](a) K. Ohno, Theor. Chim. Acta 2, 219 (1964); (b) J. M. Sichel and M. A. Whitehead, Theor. Chim. Acta 7, 32 (1967).
[16]D. W. Oxtoby and W. M. Gelbart, Mol. Phys. 29, 1569 (1975).
[17](a) W. H. Orttung, Ann. N. Y. Acad. Sci. 303, 22 (1977); (b) J. Am. Chem. Soc. 100, 4369 (1978).
[18]D. A. Long, *Raman Spectroscopy* (McGraw–Hill, New York, 1977), pp. 41–86.
[19]S. I. Chan and D. Stelman, J. Mol. Spectrosc. 10, 278 (1963).
[20]S. I. Chan, D. Stelman, and L. E. Thompson, J. Chem.

Phys. 41, 2828 (1964).
[21]S. I. Chan, J. Zinn, and W. D. Gwinn, J. Chem. Phys. 34, 1319 (1961).
[22]P. N. Skancke, G. Fogarasi, and J. E. Boggs, J. Mol. Struct. 62, 259 (1980).
[23]S. I. Chan, T. R. Borgers, J. W. Russell, H. L. Strauss, and W. D. Gwinn, J. Chem. Phys. 44, 1103 (1966).
[24]T. Ueda and T. Shimanouchi, J. Chem. Phys. 47, 4042 (1967).
[25]A. Almenningen, O. Bastiansen, and P. N. Skancke, Acta Chem. Scand. 15, 711 (1961).
[26]S. Meiboom and L. C. Snyder, J. Chem. Phys. 52, 3857 (1970).
[27]F. Takabayashi, H. Kambara, and K. Kuchitsu, in 7th Austin Symposium of Gas-Phase Molecular Structure, Austin, Texas, Paper WA6, 1978.
[28]J. S. Wright and L. Salem, Chem. Commun. 1969, 137.
[29]J. S. Wright and L. Salem, J. Am. Chem. Soc. 94, 332 (1972).
[30]L. S. Bartell and B. Andersen, Chem. Commun. 1973, 786.